Acceptance Letter

2020 IEEE 6th International Conference on Computer and Communications (ICCC)

Dec. 11-14, 2020 | Chengdu, China |

Role: **Author** (oral presentation and publication)

Paper ID: IC497

Paper Title: A Visual Based Robot Trajectory Teaching Method for Traditional Chinese Medical Moxibustion Therapy

Dear Jiaxun Liu, Qujiang Lei, Yukai Qiao, Guangchao Gui, Xiuhao Li, Jintao Jin and Weijun Wang,

Congratulations on the acceptance of your paper listed above for **2020 ICCC** Annual International Conference!

You are invited to participate and make an oral presentation in **2020 IEEE 6th International Conference on Computer and Communications (ICCC)** that will be held in **Chengdu, China** on **Dec. 11-14, 2020**. ICCC 2020 is organized by Sichuan Institute of Electronics, sponsored by IEEE, and supported by Southwest Jiaotong University, China; Sichuan University, China, etc. It is one of the leading international conferences for presenting novel and fundamental advances in the fields of computer and communication. All submissions will be peer reviewed and evaluated based on originality, technical and/or research content/depth, correctness, relevance to conference, contributions, and readability.

All accepted papers must be written in English and will be published into **conference proceedings** by IEEE. The proceedings will be submitted and reviewed by the **IEEE Xplore** and **Ei Compendex** and **Scopus** after the conference.

Attached in the letter are the reviewer's comments, plus instructions for producing the camera-ready copy, and all other necessary documents. To complete registration and include your paper in proceedings, you need to submit all required documents before the deadline. If any questions for documents preparation, then please click Guideline for Registration in the 2nd page of attached notification file.

Checking List

- ☐ **Formatted Paper (word & .pdf)**
- ☐ **Scanned and signed Confirmation Letter (.pdf)**
- ☐ **Scanned and signed copyright form (.pdf)**
- ☐ **Payment Proof (.pdf)**
- ☐ **Filled registration form(word)**
- ☐ **Scanned of student card(.pdf)/ Scanned of ieee member card(.pdf)**

Mail the above documents to iccc2015@vip.163.com before November 25, 2020.

We're looking forward to seeing you in Chengdu!

Sincerely

ICCC 2020 Conference Committees

E-mail: iccc2015@vip.163.com

Web: http://www.iccc.org/

-Guideline for Registration-

Download Link (Press Ctrl key and click on the link)

- Template: http://www.iccc.org/IEEE-Formatting.doc
- Copyright form: http://www.iccc.org/Copyright.pdf
- Confirmation letter: http://www.iccc.org/confirmation-letter.pdf
- Registration form: http://www.iccc.org/reg.docx (English/Chinese)

Camera-ready paper

- The proceedings format is 2-column with pages formatted according the standard IEEE conference style.
- The page length should be at least **full 4 pages** and better **5 pages**, or else it fails to meet publication requirement.
- The base page limit is 5 pages. Authors may buy additional pages up to 5 for **70USD or 450RMB /per page**.
- Check and confirm your acknowledgement part with your co-author or funding authority.
- Check and confirm all authors' names by order and mark a corresponding author with a "*".

Copyright consent form

You will be asked to sign an IEEE COPYRIGHT AND CONSENT FORM and send the scanned signed consent form (**pdf**):
The following blanks are all mandatory, please fill in correctly.

- TITLE OF PAPER/ARTICLE/REPORT, INCLUDING ALL CONTENT IN ANY FORM, FORMAT, OR MEDIA (hereinafter, "the Work"):
  Paper title of this accepted paper.
- COMPLETE LIST OF AUTHORS:
  All author names by order.
- 1 authorized author's signature in English and date is acceptable.
- **Please note:** Online copyright will be signed two to three weeks later after the conference. We will keep you informed.

Registration form

- 1 registration is for 1 participant only. Other authors are advised to register as listeners. Each paid registration covers only one paper; you can pay Additional Paper Fee (350.00$/2400.00￥) for one more paper from the same first author who already has a paid registration.
- One regular registration with one or more additional papers is for 1 participant only and gets only one proceeding.
- Student fee is **ONLY** applicable for students who are the FIRST authors.
- For credit card payment, sometimes if payment is failed, it is advised another e-mail should be tried again, or you can e-mail us at iccc2015@vip.163.com.
- If other payment options are required like **bank transfer (international bank account)**, the details can be requested via iccc2015@vip.163.com.

---------- Original ----------

From: "ICCC 2020"<iccc2015@vip.163.com>;
Date: Tue, Nov 24, 2020 03:08 PM
To: "qj.lei"<qj.lei@giat.ac.cn>;
Subject: ICCC 2020-IC497注册费信息

雷老师，您好：

文章IC497信息，注册费用如下：

Role: **Author** (oral presentation and publication)

Paper ID: IC497

Paper ID: A Visual Based Robot Trajectory Teaching Method for Traditional Chinese Medical Moxibustion Therapy

会议注册费合计：3700元（student regular registration）+450元(Additional Page/per one)X3=5050元

收款账户信息：

成都宗杭会展服务有限公司
账户号: 129316274303

开户行: 中国银行成都市成飞支行
联行号: 104651081260

Thanks & Best Regards.

Ms. Cynthia H. Miao | Conference Secretary

ICCC 2020 Conference Committees
2020 6th IEEE International Conference on Computer and Communications (ICCC)
Chengdu, China, December 11-14, 2020

Website: http://www.iccc.org/
E-mail: iccc2015@vip.163.com

中国建设银行网上银行电子回执

币别：人民币元　　日期：20201203　　凭证号：103297565021　　账户明细编号-交易流水号：16861-4405314070NOPAMFEHE

付款人	全 称	广州中国科学院先进技术研究所	收款人	全 称	成都宗杭会展服务有限公司
	账 号	44001531407059666666		账 号	129316274303
	开户行	中国建设银行股份有限公司广州南沙湾支行		开户行	中国银行成都成飞支行
大写金额	伍仟零伍拾元整		小写金额	5,050.00	
用 途	会议注册费		钞汇标志	钞	
摘 要	网络转账				

中国建设银行 电子回单 专用章

重要提示：银行受理成功，本回执不作为收、付款方交易的最终依据，正式回单请在交易成功第二日打印。

A Visual Based Robot Trajectory Teaching Method for Traditional Chinese Medical Moxibustion Therapy

Jiaxun Liu, Qujiang Lei, Yukai Qiao, Guangchao Gui, Xiuhao Li, Jintao Jin, Weijun Wang
Intelligent Robot & Equipment Center
Guangzhou Institute of Advanced Technology, Chinese Academy of Sciences
Guangzhou, 511458, China
Corresponding author: qj.lei@giat.ac.cn

***Abstract*—At present, Chinese traditional physiotherapy is more and more trusted and valued by people, among which moxibustion is a very effective treatment. In order to improve the efficiency of human-computer interaction and help physiotherapists to use robots to replace human power, this paper proposes a visual based robot arm trajectory teaching method. The physiotherapy staff only needs to use an optical marker to demonstrate the therapeutic trajectory on the patient's back, and the robotic arm can pick up the expected trajectory and repeat the same work. We use LK optical flow algorithm to obtain marker's motion trajectory, and then smoothen the trajectory through SG filter, which is more executable for robot arm. Finally, we design an experiment and simulate it on MATLAB to obtain the accuracy of the trajectory and the results is impressive.**

Keywords-robot, learning from demonstration, traditional Chinese medical moxibustion, machine vision, LK optical flow, trajectory optimization

I. INTRODUCTION *(HEADING 1)*

Moxibustion is a treatment method that burns moxa leaves [1] to create heat stimulating the acupuncture points or specific parts of the human body [2]. By stimulating the activity of channels and qi, it can adjust the physiological and biochemical functions of the human body [3] so as to achieve the purpose of disease prevention and treatment. The mechanism of moxibustion is similar to acupuncture, and it has complementary therapeutic effect. Moxibustion has many advantages such as simple operation, low cost and remarkable effect. But in one course of treatment, physiotherapists need to keep a certain height away from the skin to and keep moving back and forth. This repetitive motion is very tiring. In addition, the burning of moxibustion strips will produce lots of smoke, which will irritate people's eyes and respiratory tract, causing discomfort to physiotherapists. Therefore, it is necessary to use robots to replace manual labor.

Due to the repeatability and accuracy of the task, the robotic arm can be well applied to the treatment of moxibustion. At present, with increasing demand of the intelligent manufacturing mechanical arm, in order to adapt to the rapid and changeable production task in modern industry and people's life, the manipulator should not only be able to complete repeated work stably for a long time, but also need to have the characteristics of intelligence, openness and nicer man-machine cooperation. For now, there are two major problems in the research on the acquisition of the behavior and action of the robotic arm: (1) The coding process of the behavior and action based on the motion trajectory planning is relatively complicated, and the program design of the robotic arm system is complex, so the learning process of the new behavior and action is inefficient. (2) The robot arm can only move according to the planned action. When the working environment and work tasks of the robot arm is changed, the teaching behavior needs to be re-coded. The generalization ability and intelligence of the robot arm system is no very good. Therefore, as an important aspect of the continuous development and innovation of industrial robots, teaching technology is developing towards the direction that is conducive to the rapid teaching programming and the enhancement of man-machine cooperation ability.

Visual based demonstration [4][5]is a very convenient teaching tool, which can make people to plan movement tracks of the robot arm without programming foundation, and help them complete the work or life affairs. Robot can observe expected trajectory in task through the camera and then repeat the task directly. This paper introduces a visual based moxibustion trajectory teaching system. When physiotherapists demonstrate [6] the points and process of moxibustion with an optical marker, we record the track of moxibustion through a camera by using the LK optical flow method [7][8][9]. In order to reduce the vibration of the track caused by flexibility of people arm, SG filtering algorithm is used in this paper to optimize the acquired jerky trajectory and generate a smooth trajectory that is conducive to the execution of the manipulator. In the experiment, we design a test paper and print out acupoints of the tracking lines of du-arteries on the back and spine of the human body, including Great Vertebra (Du-14), Body Pillar (Du-12), Reaching Yang (Du-9), Central Pivot (Du-7), Life Gate (Du-4), and Low Back Yang Passage (Du-3).A 3D-printed optical marker moves on the corresponding target acupuncture point and records through the camera. After SG filtering, we generate a smoother trajectory. Finally, we simulate the robot arm to complete this application on MATLAB and the result is impressive.

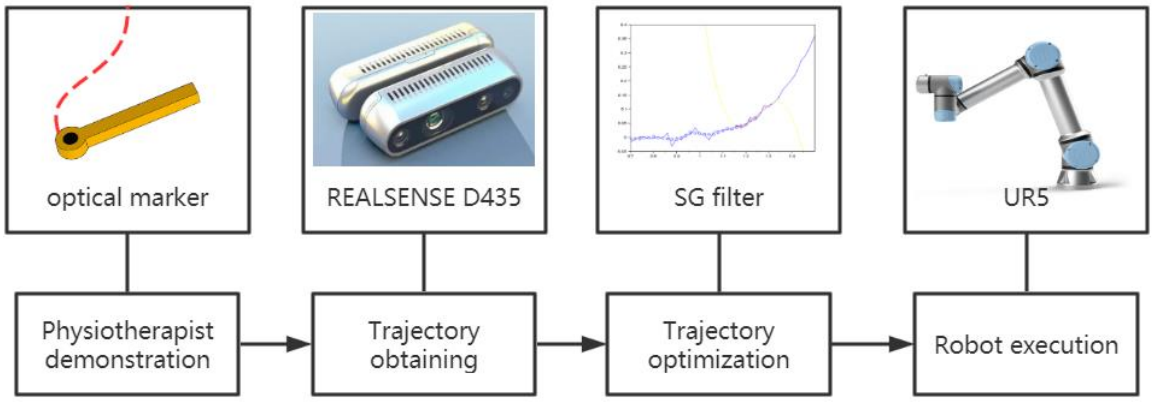

Figure 1. Workflow of the visual based robot trajectory teaching method

II. Trajectory Obtaining

In the research of vision object tracking, optical flow is a classical method. The mechanism of optical flow method is to find the corresponding relationship between the previous frame and the current frame [10] by using the change of pixels in the time domain and the correlation between adjacent frames in the image sequence [11][12], so as to calculate the motion information of objects between adjacent frames. Optical flow is the instantaneous velocity of pixels moving in space on the observed imaging plane. In general, the instantaneous change rate of gray level at a specific coordinate point of a two-dimensional image is defined as an optical flow vector [13].

To establish the optical flow method, the following two basic assumptions must be met:

(1) The assumption of constant brightness. The grayscale value (brightness) of the pixel does not change with time, which is the basic assumption of optical flow and must be met by all optical flow methods.

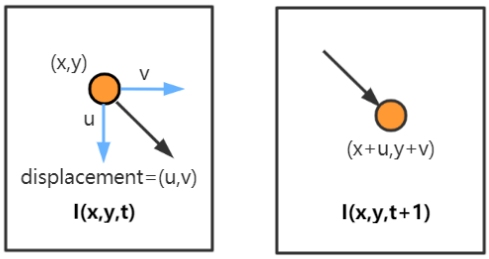

Figure 2. Diagram of constant brightness assumption

For example, the luminance value of any pixel p (x, y) in the object above (figure 2) at time t stays the same after moving (u, v) at time t +1.

(2) The assumption of "small motion". The change of time will not cause the violent change of the target position, and the displacement between the two adjacent frames is very small, so that the gray level change of the positions between adjacent frames can be used to obtain the partial derivative of the gray level position.

In order to establish the optical flow constraint equation, set the feature point pixel at moment t to be I (x, y, t), which moves dx and dy distances in the x and y directions, respectively, in dt time. According to the assumption of constant brightness:

$$I(x,y,t) = I\left(x+\mathrm{d}x, y+dy, t+\mathrm{d}t\right) \tag{1}$$

we can expand the right side of the equation by using Taylor expansion:

$$I(x,y,t) = I(x,y,t) + \frac{\partial I}{\partial x}dx + \frac{\partial I}{\partial y}dy + \frac{\partial I}{\partial t}dt + o(\partial^2) \tag{2}$$

where $o(\partial^2)$ denotes the second-order infinitesimal term, which is negligible, and brings equation (1) into equation (2) with division dt to obtain:

$$\frac{\partial I}{\partial x}\frac{dx}{dt} + \frac{\partial I}{\partial y}\frac{dy}{dt} + \frac{\partial I}{\partial t}\frac{dt}{dt} = 0 \tag{3}$$

Let u and V be the velocity vectors of the optical flow in the x and y directions, respectively:

$$u = \frac{dx}{dt}, v = \frac{dy}{dt} \tag{4}$$

set $I_x = \frac{\partial I}{\partial x}, I_y = \frac{\partial I}{\partial y}, I_t = \frac{\partial I}{\partial t}$, represents the partial derivative of pixel grayscale along x, y, and t， respectively, then equation (3) can be written as follows：

$$I_x u + I_y v + I_t = 0 \tag{5}$$

According to equation (5), there is only one optical flow constraint equation but two unknowns, so the exact value cannot be obtained, and other constraints need to be introduced to solve the equation. Therefore, different optical flow methods are formed by solving the optical flow constraint equation with different constraints introduced from different angles.

In the development of optical flow, the two most classic gradient-based optical flow algorithms are HS global optical flow (dense optical flow) and LK local optical flow (sparse optical flow). Generally, only one moxibustion strip is needed for physiotherapy, so the LK optical flow method is used for simple tracking of a single optical maker in this paper. The LK optical flow method is proposed by Bruce D. Lucas and Takeo Kanade. In addition to meeting the requirement of constant brightness and small motion, the LK optical flow method also needs to meet the requirement of uniform space. Spatial consistency means two pixels adjacent to each other on the previous frame and also adjacent to each other on the next frame.

Within a neighborhood, calculate weighted squared and minimized to estimate the optical flow vector for the following equation.

$$\sum_{(x,y\in\Omega)} W^2(x)(I_x u + I_y v + I_t)^2 \tag{6}$$

where $W^2(x)$ denotes the neighborhood window Ω weighting function, which typically makes the neighborhood center weighted larger than the neighborhood. For n points $X_1, X_2 \ldots X_n$ within the neighborhood Ω $X_1, X_2 \ldots X_n$, set：

$$V = (u,v)^T, \nabla I(X) = (I_x, I_y)^T \tag{7}$$

set $A = \begin{pmatrix} I_x(X_1) & I_y(X_1) \\ \vdots & \vdots \\ I_x(X_n) & I_y(X_n) \end{pmatrix}$

$$W = \begin{pmatrix} W(X_1) & 0 & 0 & 0 \\ 0 & W(X_2) & 0 & 0 \\ \vdots & \vdots & \ddots & \vdots \\ 0 & 0 & 0 & W(X_N) \end{pmatrix} \quad b = \begin{pmatrix} I_t = (X_1) \\ I_t = (X_2) \\ \vdots \\ I_t = (X_n) \end{pmatrix}$$

The least squares method is used to approximate the solution:

$$A^T W^2 A V = A^T W^2 b \tag{8}$$

and the optical flow vector V is：

$$V = (A^T W^2 A)^{-1} A^T W^2 b \tag{9}$$

$$V = \begin{pmatrix} u \\ v \end{pmatrix} = \begin{pmatrix} \sum W^2 I_x^2 & \sum W^2 I_x I_y \\ \sum W^2 I_x I_y & \sum W^2 I_y^2 \end{pmatrix} \begin{pmatrix} -\sum W^2 I_x I_t \\ -\sum W^2 I_y I_t \end{pmatrix} \tag{10}$$

The above calculations are performed in the window field Ω. By combining information from a few nearby pixels, the LK optical flow method can eliminate polynomial in the optical flow equation.

III. TRAJECTORY OPTIMIZATION

Due to flexible wrists, when people demonstrate expected trajectory, the trail recorded by optical flow tend to contain many jagged parts. Although there are lots of classical methods such as FIR filter [14] and Kalman Smoother [15] applied to eliminate random noise, the SG filter outperforms them in approximating the true trajectory [16]. In order to reduce the impact of hand shaking and approach demonstration path as far as possible, this paper optimizes and generates a trajectory that is conducive to the execution of the manipulator [17] through SG smoothing algorithm.SG smoothing algorithm is a least square based polynomial smoothing algorithm proposed by Abraham Savitzky and Marcel J. E. Golay, also known as convolution smoothing.

The key to Savitzky-Golay convolution smoothing lies in the solution of matrix operator.

Set the width of the filter window to$n = 2m + 1$, and each measurement point is:

$$x = (-m, -m+1, 0 \ldots 0, 1, \ldots m-1, m)$$

Fitting of data points within a window by using k-1st polynomial:

$$y = a_0 + a_1 x + a_2 x^2 + \cdots + a_{k-1} x^{k-1} \tag{11}$$

So, there are n such equations, fastened into a k-element linear group of equations. For a set of equations to have a solution then n should be greater than or equal to k. The general choice is n>k, through the least-squares legal fit parameter A. This gives:

$$\begin{pmatrix} y_{-m} \\ y_{-m-1} \\ \vdots \\ y_m \end{pmatrix} = \begin{pmatrix} 1 & -m & \cdots & (-m)^{k-1} \\ 1 & -m+1 & \cdots & (-m+1)^{k-1} \\ \vdots & \vdots & \ddots & \vdots \\ 1 & m & \cdots & m^{k-1} \end{pmatrix} \begin{pmatrix} a_0 \\ a_1 \\ \vdots \\ a_{k-1} \end{pmatrix} + \begin{pmatrix} e_{-m} \\ e_{-m+1} \\ \vdots \\ e_m \end{pmatrix} \tag{12}$$

Expressed as a matrix:

$$Y_{(2m+1)\times 1} = X_{(2m+1)\times k} \cdot A_{K\times 1} + E_{(2m+1)\times 1} \tag{13}$$

The least-squares solution $\dot{A}$ of A is:

$$\dot{A} = (X^T \cdot X)^{-1} \cdot X^T \cdot Y \tag{14}$$

The model predictions or filtered values of Y are:

$$\dot{Y} = X \cdot A = X \cdot (X^T \cdot X)^{-1} \cdot X^T \cdot Y = B \cdot Y \tag{15}$$

$$B = X \cdot (X^T \cdot X)^{-1} \cdot X^T \tag{16}$$

In this passage, we use the five-point cubic smoothing formula, where the five points at equal wavelength intervals in a section of the spectrum are referred to as the X-set. Polynomial smoothing uses polynomial fits to data at wavelength points Xm-2, Xm-1, Xm, Xm+1, Xm+2 instead of Xm, and then moves them around until the spectrum is traversed (figure 3).

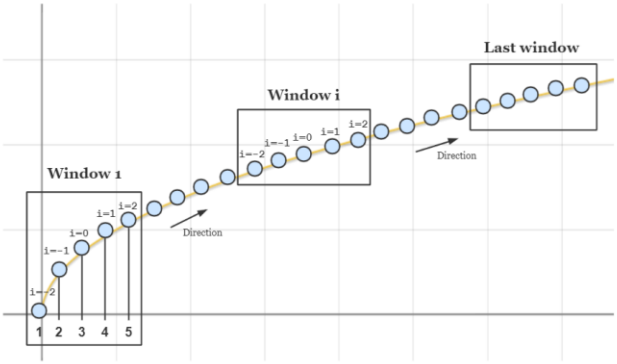

Figure 3. 5-point quadratic polynomial smoothing mechanism

If we take m=2, k=4，then we get the cubic polynomial：

$$Y = a_0 + a_1 x + a_2 x^2 + a_3 x^3$$

According to the least-squares principle, the coefficients a0, a1, a2, a3 are determined, and the final five-point cubic smoothing formula is as follows：

$$\bar{Y}_{-2} = \frac{1}{70}(69Y_{-2} + 4Y_{-1} - 6Y_0 + 4Y_1 - Y_2) \tag{17}$$

$$\bar{Y}_{-1} = \frac{1}{35}(2Y_{-2} + 27Y_{-1} + 12Y_0 - 8Y_1 + 2Y_2) \tag{18}$$

$$\bar{Y}_0 = \frac{1}{35}(-3Y_{-2} + 12Y_{-1} + 17Y_0 + 12Y_1 - 3Y_2) \tag{19}$$

$$\bar{Y}_1 = \frac{1}{35}(2Y_{-2} - 8Y_{-1} + 12Y_0 + 27Y_1 + 2Y_2) \tag{20}$$

$$\bar{Y}_2 = \frac{1}{70}(-Y_{-2} + 4Y_{-1} - 6Y_0 + 4Y_1 + 69Y_2) \tag{21}$$

where $\bar{Y}_i$ is the improved value of Y_i .

The formula requires data points n ≥5, and when there are more than 5 data points, for symmetry considerations, the rest are smoothed by formula (19) except at the ends with formulae (17), (18) and (20), (21), respectively, which is equivalent to smoothing with a different triple least squares polynomial on each subinterval.

IV. EXPERIMENT

A. *Experiment components*

The experiment components consist of a REALSENCE D435 camera mounted on a shelf above the work platform, an optical marker, and one test paper of acupoints in human's back.

The governor meridian in the back and spine of human body contains important acupoints in moxibustion therapy. In the experiment, according to the meridian diagram in the Figure 4, we extract the acupoints of Great Vertebra (Du-14), Body Pillar (Du-12), Reaching Yang (Du-9), Central Pivot (Du-7), Life Gate (Du-4), and Low Back Yang Passage (Du-3) successively from the top to the bottom as the test object of demonstration and print it out as a test paper (figure 5) .

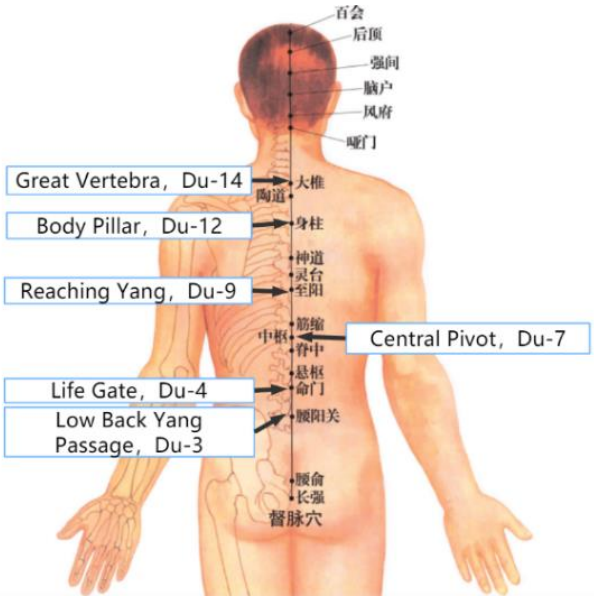

Figure 4. Acupuncture point of human spine

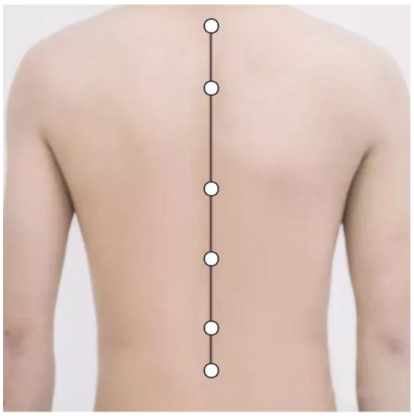

Figure 5. Extracted acupoints for experiments

We also use 3D printer to print out a little optical marker showed in figure 6 and the black circle is considered as the object for the trajectory tracking.

Figure 6. Optical marker

B. Experiment steps

In the experiment, we first obtain the position of the acupuncture point theoretically in the image taken from the camera as shown in Figure 7, and take it as the standard to test the trajectory accuracy.

In moxibustion therapy, physiotherapist must pay attention to the accuracy of acupoints and physical comfort. In order to achieve the desired effect [18][19][20], in addition to finding the acupuncture points according to the prescription, moxibustion usually requires reciprocating or circumferential movements around the acupuncture points, so as to avoid discomfort caused by excessive temperature. Therefore, we design the moxibustion route from the Great Vertebra (Du-14) to the Low Back Yang Passage (Du-3), which includes some reciprocating and circling routes. After setting the black dot in the middle of optical marker as the tracking point of optical flow, as shown in Figure 8, we manually operate optical marker to complete the previously planned moxibustion route, as shown in Figure 9.

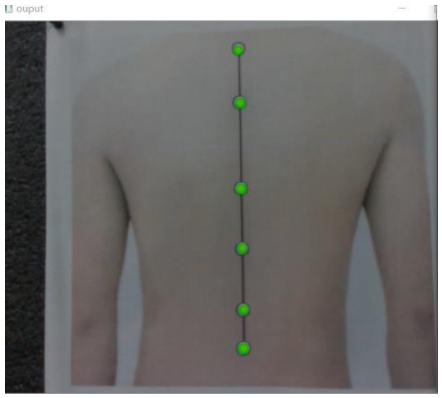

Figure 7. Standard locations of acupoints acquired in camera images

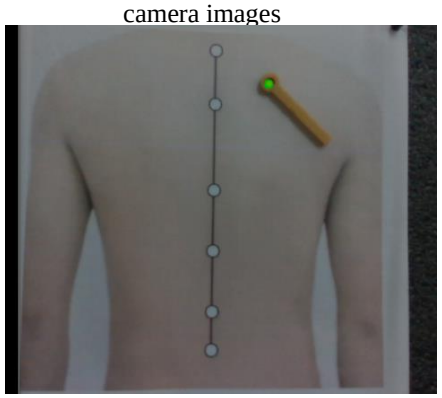

Figure 8. The tracking point of the optical marker acquired in the camera image

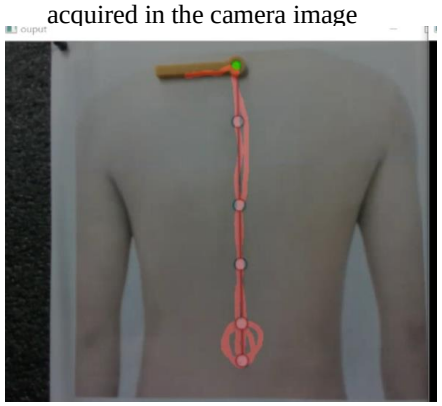

(a)

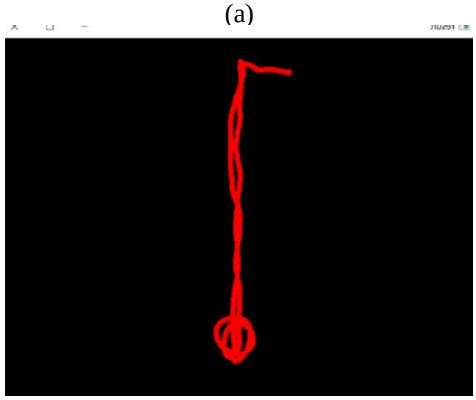

(b)

Figure 9. Teaching trajectory acquired under the camera

We record 15 teaching trajectories in experiment (as shown in Figure 10) and then smoothed the acquired trajectories by using SG filtering. The comparison of the original trajectory diagram and the smoothed trajectory diagram is shown in the figure 11. It can be seen that the jerky part of the circling routes becomes smoother and the reciprocating route becomes straighter.

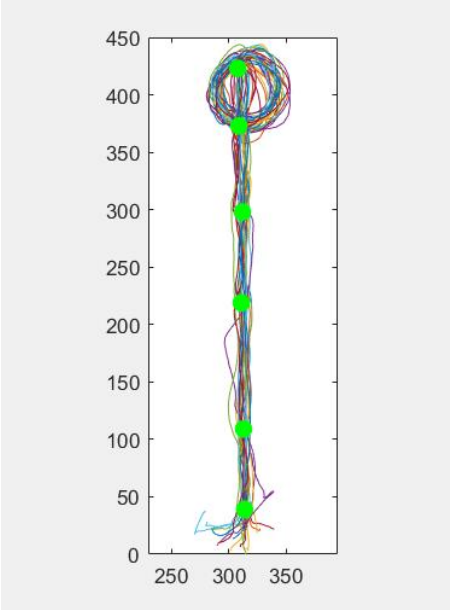

Figure 10. 15 teaching trajectories

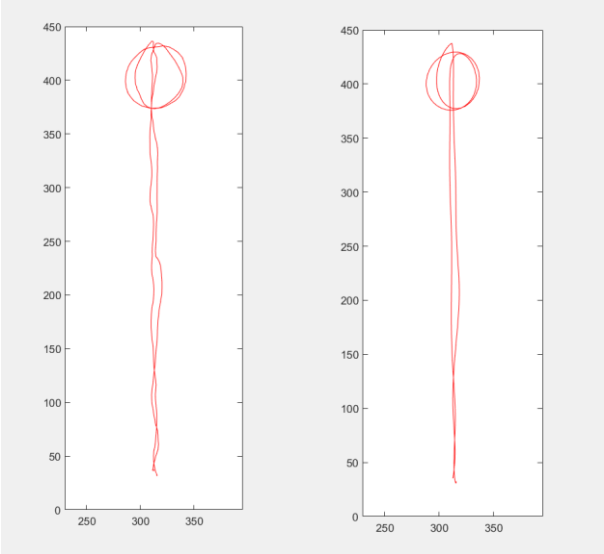

(a) Original trajectory (b) Smoothed trajectory

Figure 11. Comparison of the original trajectory diagram and the smoothed trajectory

C. *Result*

In order to prove the accuracy of the acquired trajectory, we design the standard to test accuracy of the tracks. According to [21], the author randomly selects 71 experienced physicians and record the locations of their treatment points. The mean area of 95% and 68% confidence intervals range of the acupoints in the treatment is 19.4 cm^2 and 4.8 cm^2 , respectively. Therefore, to determine the effectiveness of the trajectory sheet, we set up three round areas of acupoint. Taking the theoretical acupoint position as the center of the circle, we set up 3 standard circular range for the acupoints in the treatment and the diameter of the circle area is 4 cm, 3cm and 2cm, respectively.

In the experiment, the men on the test paper have a shoulder width of 15cm and the average adult male in China has a shoulder width of 37.5cm. Assuming that the males in the experimental paper represented the average Chinese adult males, the 3 standard circular treatment areas which we have introduced should be changed to 3 circular areas with diameters of 1.6cm,1.2 cm and 0.8cm in accordance with the corresponding proportions. We simulate these standards on MATLAB, as shown in figure 12.

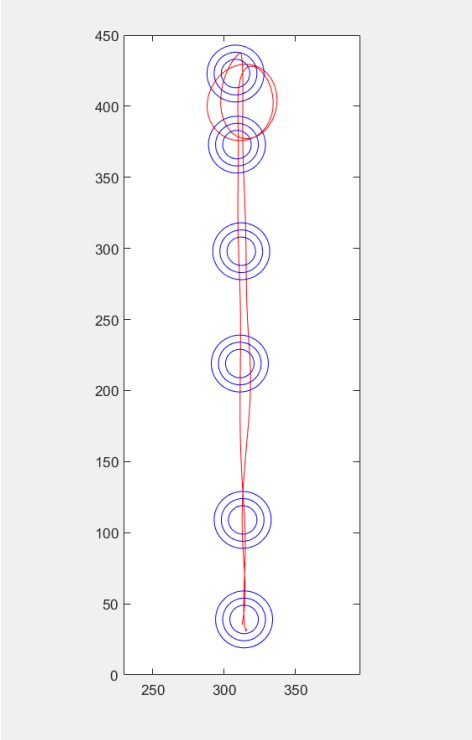

Figure 12. Diagram of the three ranges of acupoints

These three ranges represent different teaching accuracy standards. If the teaching path intersects the circle, the teaching is deemed successful; if it does not intersect the circle, the teaching is deemed unsuccessful. The accuracy of the teaching curve can be known from the number of successes and failures. According to figure 12, the number of times the trajectory theory should pass through the acupuncture point should be 15, and there are 15 intersecting line segments within the maximum circle range,

so the accuracy rate is 100%. With this method, we calculate the accuracy of 15 trajectories according to different accuracy standards, as shown in table 1.

No.	Standard1	Standard2	Standard3
1	100%	100%	100%
2	100%	100%	100%
3	100%	100%	93.3%
4	100%	100%	100%
5	100%	90.9%	81.8%
6	100%	100%	90.0%
7	100%	90.0%	90.0%
8	100%	93.3%	93.3%
9	100%	90.9%	90.9%
10	100%	100%	100%
11	100%	100%	91.6%
12	100%	100%	100%
13	100%	100%	100%
14	100%	100%	85.7%
15	100%	92.3%	84.6%
Average	100%	97.16%	93.36%

Table 1. Accuracy of trajectories under three criteria

In terms of the average success rate, the expected trajectory generated by this method will not exceed the deviation of 2cm from the physiotherapy acupuncture point, and the accuracy within the range of 1cm from the acupuncture point is over 90%, which achieves the expected effect comparing with artificial moxibustion.

V. CONCLUSION

In this paper, we design a visual based teaching method for moxibustion therapy, so that it can avoid complex programming and simplify the process for physiotherapists to operate robot arms, contributing to the development of medical service. Through the LK optical flow method, we can capture the position of optical Marker and generate its locus. The trajectory is then smoothed through SG filtering. Finally, in the experiment, the accuracy rate of the trajectory reaches 93.36% within the range of 1cm around the theoretical acupuncture point, achieving the expected effect.

FUTURE WORK

In this paper, trajectory teaching on 2D plane is mainly studied. Generally, during physiotherapy, people will lie down and stay still. Although this method can ensure the therapeutic effect by setting the height of the end of the robot arm, a more convenient and accurate method is to directly acquire 3D trajectory for demonstration. Moreover, in the research of trajectory optimization, the key position of the actual acupuncture point is not known during the smooth process, due to lack of certain constraints. In the future, we will study trajectory tracking methods in three-dimensional space and better trajectory optimization method to improve the accuracy of the trajectory.

ACKNOWLEDGMENT

This research is supported by the Major Projects of Guangzhou City of China (Grant No. 201907010012).

REFERENCES

[1] S. Pal, C. Mitra and D. Bakshi, "Development of Moxibustion based novel technique using Himalayan herbs for fast relief as well as prevention of certain human ailments," 2010 International Conference on Systems in Medicine and Biology, Kharagpur, 2010, pp. 309-312, doi: 10.1109/ICSMB.2010.5735393.

[2] Seung-Ho Yi, Thermal Properties of Direct and Indirect Moxibustion, Journal of Acupuncture and Meridian Studies, Volume 2, Issue 4,2009,Pages 273-279,ISSN 2005-2901,https://doi.org/10.1016/S2005-2901(09)60068-6.

[3] H. Zhen, L. Dongyu and L. Chengwei, "Implementation of Reinforcement and Reduction of Traditional Acupuncture and Moxibustion," 2008 International Conference on BioMedical Engineering and Informatics, Sanya, 2008, pp. 522-525, doi: 10.1109/BMEI.2008.99.

[4] Rahmatizadeh R , Abolghasemi P , Bölöni, Ladislau, et al. Vision-Based Multi-Task Manipulation for Inexpensive Robots Using End-To-End Learning from Demonstration[J]. 2017.

[5] Yu T , Abbeel P , Levine S , et al. One-Shot Composition of Vision-Based Skills from Demonstration[C]// 2019 IEEE/RSJ International Conference on Intelligent Robots and Systems (IROS). IEEE, 2020.

[6] Das N , Prakash R , Behera L . Learning object manipulation from demonstration through vision for the 7-DOF barrett WAM[C]// IEEE First International Conference on Control. IEEE, 2016

[7] G. Han, X. Li, N. Sun and J. Liu, "A robust object detection algorithm based on background difference and LK optical flow," 2014 11th International Conference on Fuzzy Systems and Knowledge Discovery (FSKD), Xiamen, 2014, pp. 554-559, doi: 10.1109/FSKD.2014.6980894.

[8] Q. Dao Vu and S. Chung, "Real-time robust human tracking based on Lucas-Kanade optical flow and deep detection for embedded surveillance," 2017 8th International Conference of Information and Communication Technology for Embedded Systems (IC-ICTES), Chonburi, 2017, pp. 1-6, doi: 10.1109/ICTEmSys.2017.7958761.

[9] L. Dan, J. Dai-Hong, B. Rong, S. Jin-Ping, Z. Wen-Jing and W. Chao, "Moving object tracking method based on improved lucas-kanade sparse optical flow algorithm," 2017 International Smart Cities Conference (ISC2), Wuxi, 2017, pp. 1-5, doi: 10.1109/ISC2.2017.8090850.

[10] Blu T , Moulin P , Gilliam C . Approximationorder of the lap optical flow algorithm[C]// 2015 IEEE International Conference on Image Processing (ICIP). IEEE, 2015.

[11] H. Zhang, L. Xiao and G. Xu, "A Novel Tracking Method Based on Improved FAST Corner Detection and Pyramid LK Optical Flow," 2020 Chinese Control And Decision Conference (CCDC), Hefei, China, 2020, pp. 1871-1876, doi: 10.1109/CCDC49329.2020.9164332.

[12] Kale K , Pawar S , Dhulekar P . Moving object tracking using optical flow and motion vector estimation[C]// International Conference on Reliability. IEEE, 2015.

[13] M. P. Patel and S. K. Parmar, "Moving object detection with moving background using optic flow," International Conference on Recent Advances and Innovations in Engineering (ICRAIE-2014), Jaipur, 2014, pp. 1-6, doi: 10.1109/ICRAIE.2014.6909190.

[14] G. Xia, X. Xia, B. Zhao, C. Sun, P. Wang and Y. yang, "A Method of Online Trajectory Generation Based on FIR Filter," 2019 Chinese Automation Congress (CAC), Hangzhou, China, 2019, pp. 919-924, doi: 10.1109/CAC48633.2019.8996311.

[15] Kuronen, Toni. Post-processing and analysis of tracked hand trajectories[J]. 2014.

[16] Liu, Yang & Dang, Bo & Li, Yue & Lin, Hongbo & Ma, Haitao. (2015). Applications of Savitzky-Golay Filter for Seismic Random Noise Reduction. Acta Geophysica. 64. 10.1515/acgeo-2015-0062.

[17] R. Yadav and B. K. Rout, "Trajectory Optimization of Continuum arm robots," 2019 28th IEEE International Conference on Robot and Human Interactive Communication (RO-MAN), New Delhi, India, 2019, pp. 1-6, doi: 10.1109/RO-MAN46459.2019.8956407.

[18] Z. Chen, G. Jiang and C. Huang, "Numerical simulation of moxibustion therapy based on simplified heat transfer model," 2010 3rd International Conference on Biomedical Engineering and Informatics, Yantai, 2010, pp. 1232-1235, doi: 10.1109/BMEI.2010.5639286.

[19] S. Nakamura, M. Nakamura, E. Maeda and Y. Nikawa, "Noninvasive temperature measurement during moxibustion using MRI," Asia-Pacific Microwave Conference 2011, Melbourne, VIC, 2011, pp. 594-597.

[20] T. Shen, "Technology Developments in Acupuncture and Moxibustion Treatment [Commentary]," in IEEE Technology and Society Magazine, vol. 36, no. 4, pp. 21-22, Dec. 2017, doi: 10.1109/MTS.2017.2763443.

[21] Molsberger A F , Manickavasagan J , Abholz H H , et al. Acupuncture points are large fields: The fuzziness of acupuncture point localization by doctors in practice[J]. European Journal of Pain, 2012, 16(9):1264-1270.